Landau levels with magnetic tunneling in a Weyl semimetal and magnetoconductance of a ballistic *p-n* junction

D. R. Saykin,[1,2] K. S. Tikhonov,[2,3,4] and Ya. I. Rodionov[3,5]

[1]*Moscow Institute of Physics and Technology, Moscow 141700, Russia*
[2]*L. D. Landau Institute for Theoretical Physics, Chernogolovka 142432, Russia*
[3]*National University of Science and Technology MISIS, Department of Theoretical Physics
and Quantum Technologies, Moscow 119049, Russia*
[4]*Physics Department, Moscow State University of Education, Moscow 119992, Russia*
[5]*Institute for Theoretical and Applied Electrodynamics, Moscow 125412, Russia*

We study the Landau levels (LLs) of a Weyl semimetal with two adjacent Weyl nodes. We consider different orientations $\eta = \angle(\mathbf{B}, \mathbf{k}_0)$ of magnetic field $\mathbf{B}$ with respect to $\mathbf{k}_0$, the vector of Weyl node splitting. A magnetic field facilitates the tunneling between the nodes, giving rise to a gap in the transverse energy of the zeroth LL. We show how the spectrum is rearranged at different η and how this manifests itself in the change of behavior of the differential magnetoconductance $dG(B)/dB$ of a ballistic *p-n* junction. Unlike the single-cone model where Klein tunneling reveals itself in positive $dG(B)/dB$, in the two-cone case, $G(B)$ is nonmonotonic with a maximum at $B_c \propto \Phi_0 k_0^2 / \ln(k_0 l_E)$ for large $k_0 l_E$, where $l_E = \sqrt{\hbar v / |e|E}$, with E for the built-in electric field and Φ_0 for the magnetic flux quantum.

I. INTRODUCTION

Since the discovery of time-reversal invariant topological insulators (see Ref. [1] and references therein) the topological properties of the electronic band structure of crystalline materials have been enjoying a lot of attention. After Ref. [2] indicated the possibility of a Weyl semimetal (WSM) state for pyrochlore iridates, the quest for model Hamiltonians and material candidates ensued [3–6].

The WSM state was first discovered in TaAs [7,8] and TaP [9]. First-principles calculations [10,11] (confirmed by later experiments) revealed that in both materials all Weyl nodes form a set of closely positioned pairs of opposite chirality in momentum space. Recently, active experimental research [12–17] shifted from the initial band-structure study to the surface and transport phenomena: A significant amount of attention was devoted to magnetotransport, which was addressed theoretically [18–21] and experimentally [22–25].

One of the manifestations of the gapless band structure is Klein tunneling, which reveals itself in transport through a *p-n* junction. The recent study in Ref. [20] was devoted to the magnetoconductance of a *p-n* junction realized in WSM. The authors showed that in the case of a longitudinally aligned external magnetic field, $\mathbf{B} \parallel \mathbf{E}$, where $\mathbf{E}$ is a junction's built-in electric field, the differential magnetoconductance $dG(B)/dB$ is positive. This situation is opposite from the ordinary semiconductor *p-n* junction [26–28].

The treatment of Ref. [20] was done in the approximation of well-separated (in momentum space) Weyl nodes. Usually, the influence of a pairwise [29] structure of WSM nodes on transport phenomena is accounted for by the simple multiplication of a single point contribution by the number of cones in the spectrum. This approach, however, breaks down in strong magnetic fields. When the cyclotron radius of a particle

$R_c \sim \hbar c k_0 / |e| B$ with momentum k_0 becomes of the order of its coordinate uncertainty k_0^{-1}, internode coupling must be taken into account. For example, in TaAs [8] the momentum distance between the Weyl nodes in a pair is $2k_0 = 0.0183 \, \text{Å}^{-1}$ and it happens at fields of order $B \simeq \Phi_0 k_0^2 \simeq 17$ T. Indeed, such field-induced tunneling between two nodes in a pair has already been observed experimentally [30]. Since the distance between the pairs of Weyl nodes is usually much larger than the internode distance inside a pair, we consider the nodes to be pairwise. A generic low-energy Hamiltonian for such a system was derived in Ref. [31],

$$\mathcal{H} = \Delta + \frac{\hbar^2}{2m}(\hat{k}_x^2 - k_0^2)\sigma_x + \hbar v(\hat{k}_y \sigma_y + \hat{k}_z \sigma_z), \quad (1)$$

where Δ is the Weyl node energy measured from the chemical potential and v stands for the Fermi velocity. In what follows, we drop out the energy offset Δ (it only matters in the estimation of a heterojunction's built-in potential [20]).

The problem of field-induced internode tunneling was addressed in a semiclassical approximation [32]. Recently, the same problem was analyzed numerically for a magnetic field perpendicular to the node splitting [30,33], and the angular dependence has been studied within the *ab initio* tight-binding model [34]. It was discovered that magnetically induced tunneling opens a gap in a Landau level (LL) zeroth mode.

In the framework of a model described by Hamiltonian Eq. (1), our results are as follows. We present an analytical theory of the spectrum of the LLs and its dependence on angle η between the magnetic field $\mathbf{B}$ and $\mathbf{k}_0$. In particular, we show that for $\eta = \pi/2$ the problem of LLs is reduced to the supersymmetric quantum mechanics of a particle in a quadratic superpotential. The lowest LL energy is indeed exponentially
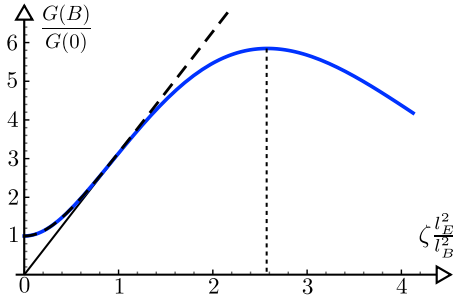
FIG. 1. Magnetoconductance $\frac{G(B)}{G(0)}$ vs dimensionless magnetic field $\zeta \frac{vB}{cE}$ plotted from Eq. (18) with parameter $\zeta k_0 l_E = 2$. The dashed line represents the result of Ref. [20] and the black line depicts first term of the sum (17).

close to zero and nonperturbative in the magnetic field,

$$\varepsilon_0 = \frac{(\hbar k_0)^2}{m}\sqrt{\frac{B}{\pi B_0}}\exp\left(-\frac{2B_0}{3B}\right), \quad B_0 = \zeta\frac{\Phi_0 k_0^2}{\pi}, \quad (2)$$

where $\zeta \equiv \frac{v_x}{v_y} = \frac{\hbar k_0}{mv}$ is the anisotropy parameter. The numerically computed dependence of LLs on angle η between the magnetic field $\mathbf{B}$ and $\mathbf{k}_0$ is shown in Fig. 3.

We have also studied the magnetoconductance of a WSM-based ballistic p-n junction for $\mathbf{E} \parallel \mathbf{B} \perp \mathbf{k}_0$ and found that the magnetoconductance becomes a nonmonotonic function of B (see Fig. 1). We found the field corresponding to the maximum of $G(B)$ to be

$$B_c \sim \frac{2}{3}\frac{B_0}{\ln(\zeta k_0 l_E)}, \quad \zeta k_0 l_E \gg 1, \quad (3)$$

where $l_E = \sqrt{\hbar v/|e|E}$ is the built-in electric field length.

This Rapid Communication is organized as follows: Section II explores the structure of LLs in the two-conical system of Eq. (1), Sec. III is dedicated to the magnetoconductance of a ballistic p-n junction realized in such a system, and the conclusions are drawn in Sec. IV.

II. LANDAU LEVELS

We begin our analysis with the search for an energy dispersion law in the presence of the magnetic field starting from Hamiltonian (1). We orient the coordinates so that the x axis points in the direction of the Weyl node separation $\mathbf{k}_0$. The magnetic field $\mathbf{B} = B(\cos\eta, 0, \sin\eta)$ is inclined at an angle η with respect to the x axis (see the Supplemental Material [35] for an illustration), so that the field is described by the potential $\mathbf{A} = B(-y\sin\eta, 0, y\cos\eta)$. At first, we solve an eigenvalue problem in two limiting cases $\eta = 0, \frac{\pi}{2}$ analytically and then provide numerical solutions for arbitrary angles.

Field parallel to node splitting. We start from the case $\eta = \angle(\mathbf{B}, \mathbf{k}_0) = 0$. After the shift of the variable $y \mapsto y - k_z l_B^2$, where $l_B = \sqrt{\hbar c/|e|B}$ is the magnetic length, and the unitary rotation $\psi \mapsto \frac{1}{\sqrt{2}}(1 + i\sigma_y)\psi$, the Hamiltonian transforms to

$$\mathcal{H} = \hbar v \begin{pmatrix} -\frac{\hbar}{2mv}(k_x^2 - k_0^2) & yl_B^{-2} - \partial_y \\ yl_B^{-2} + \partial_y & \frac{\hbar}{2mv}(k_x^2 - k_0^2) \end{pmatrix}. \quad (4)$$
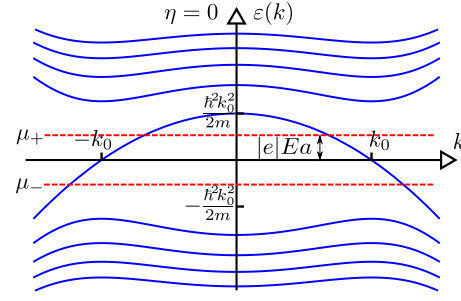
FIG. 2. Landau levels for $\eta = \angle(\mathbf{B}, \mathbf{k}_0) = 0$ plotted from Eq. (6). The magnetic field is supposed to satisfy $l_B a < l_E^2$ and electrochemical potentials from different sides of the junction are noted as $\mu_{\pm} = \mu(\pm\infty)$.

Eigenfunctions are expressed through the Hermite functions $\psi_n^{\text{osc}}(y) = (2^n n!\sqrt{\pi}l_B)^{-1/2}e^{-y^2/2}H_n(y)$ as

$$\psi_{n\neq 0} = \begin{pmatrix} c_n^1\psi_{|n|}^{\text{osc}}(yl_B^{-1}) \\ c_n^2\psi_{|n|-1}^{\text{osc}}(yl_B^{-1}) \end{pmatrix}, \quad \psi_0 = \begin{pmatrix} \psi_0^{\text{osc}}(yl_B^{-1}) \\ 0 \end{pmatrix}, \quad (5)$$

where $n \in \mathbb{Z}$ and coefficients c_n^i are determined as eigenvectors of (4) with $\sqrt{2|n|}/l_B$ instead of $yl_B^{-2} \pm \partial_y$. As a result, we find

$$\varepsilon_{n\neq 0}(k_x) = \hbar v\,\text{sgn}(n)\sqrt{\frac{2|n|}{l_B^2} + \left(\frac{\hbar(k_x^2 - k_0^2)}{2mv}\right)^2},$$

$$\varepsilon_0(k_x) = -\frac{\hbar^2}{2m}(k_x^2 - k_0^2), \quad n \in \mathbb{Z}. \quad (6)$$

We present the plot of LLs in Fig. 2. It is important to note that the zeroth LL is independent of magnetic field. It leads to a linear-in-B magnetoconductance $G(B)$ for large B in such an orientation (see Sec. III). A similar scheme of LLs was obtained in Ref. [36] for $\eta = 0$ and an almost identical Hamiltonian.

Field perpendicular to node splitting. For the case $\eta = \angle(\mathbf{B}, \mathbf{k}_0) = \frac{\pi}{2}$, after the shift $y \mapsto y + k_x l_B^2$, the Hamiltonian becomes

$$\mathcal{H} = \hbar v \begin{pmatrix} k_z & Q \\ Q^{\dagger} & -k_z \end{pmatrix}, \quad Q = W(y) - i\widehat{p}_y. \quad (7)$$

Hamiltonian (7) can be analyzed in terms of supersymmetric quantum mechanics where the function $W(y) = \frac{\hbar}{2mv}(y^2 l_B^{-4} - k_0^2)$ plays the role of a superpotential. To find the eigenvectors one may factorize the y-dependent part of the ψ function as the solution of

$$\begin{array}{l} Q\chi_n^2 = -l_B^{-1}\epsilon_n\chi_n^1 \\ Q^{\dagger}\chi_n^1 = -l_B^{-1}\epsilon_n\chi_n^2 \end{array}, \quad \psi_n = \begin{pmatrix} c_n^1\chi_{|n|}^1(\frac{y}{l_B}) \\ c_n^2\chi_{|n|}^2(-\frac{y}{l_B}) \end{pmatrix}. \quad (8)$$

When $\chi_n^{1,2}(y)$ is found, vectors c_n can be determined from $\mathcal{H}c_n = \epsilon_n c_n$ with Q and Q^+ replaced with $-\epsilon_{|n|}$. Transverse energies then are given by

$$\varepsilon_n(k_z) = \hbar v\,\text{sgn}(n)\sqrt{\frac{\epsilon_{|n|}^2}{l_B^2} + k_z^2}, \quad n = \pm 0, \pm 1, \ldots, \quad (9)$$

where ± 0 denotes the ground states for electrons and holes, respectively, with the convention $\text{sgn}(\pm 0) = \pm 1$.
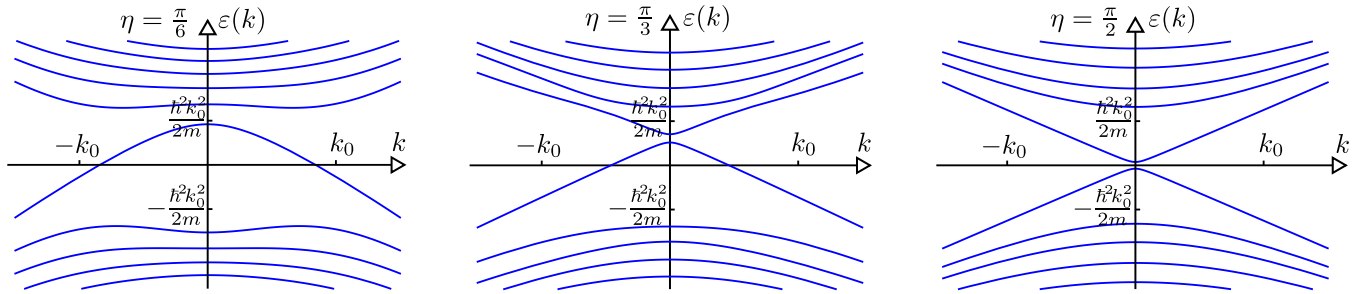
FIG. 3. Energy vs momentum along the magnetic field $\mathbf{k} \parallel \mathbf{B}$ dependence (computed numerically) with parameters $\zeta = 1.6$ and $k_0 l_B = 1.4$ for different angles $\eta = \pi/6, \pi/3, \pi/2$. Material parameters are taken for TaAs, $\hbar^2 k_0^2/2m \simeq 12$ meV, and the magnetic field is set to $B \simeq 34$ T to make the gap visible at $\eta = \pi/2$.

We still have to solve the eigenproblem (8) to determine ϵ_n. The spectrum of the problem can be found analytically for $k_0 l_B \gg 1$. In the limit of $k_0 \to +\infty$ with ζ fixed, the Weyl cones become separated and the ψ function near each Weyl point is given [20] by an appropriate combination of Hermite functions $\psi_n^{\mathrm{osc}}(y)$ with $\epsilon_n = \sqrt{2\zeta n}$. To solve the present problem, we introduce a coupling constant $g \equiv (4\zeta k_0^2 l_B^2)^{-1} \ll 1$ and rescale $y \mapsto y/\sqrt{\zeta}$. Using Eq. (11) we write down the corresponding Schrödinger equation,

$$\left[-\partial_y^2 + g\left(y^2 - \frac{1}{4g}\right)^2 \mp 2\sqrt{g}\, y \right] \chi^{1,2} = 2\nu \chi^{1,2}, \quad (10)$$

where we denoted $2\nu \equiv \epsilon_n^2/\zeta$. For $g \to 0$ we have two independent harmonic oscillators with eigenvalues $\nu_n = \lceil \frac{n}{2} \rceil$, $n \in \mathbb{N}_0$ (so that $\nu_0 = 0$, $\nu_1 = \nu_2 = 1$, $\nu_3 = 2$, etc.).

Let us show that at small g there are no perturbative corrections to the ground-state energy of Eq. (10). To this end, it is convenient to reconsider the original Eqs. (8) and decouple them via

$$Q^\dagger Q \chi_n^1 = \left(\frac{\epsilon_n}{l_B}\right)^2 \chi_n^1, \quad Q Q^\dagger \chi_n^2 = \left(\frac{\epsilon_n}{l_B}\right)^2 \chi_n^2. \quad (11)$$

Thus, we obtained Schrödinger equation (10) with a supersymmetric potential [37]. One can thus try to construct an exact ground state of $Q^\dagger Q$,

$$Q \chi_0(y) = 0 \Leftrightarrow \chi_{\epsilon=0} = \exp\left(-\frac{y_+^2}{2} - \sqrt{g}\,\frac{y_+^3}{3} \right), \quad (12)$$

where $y_+ = y - \frac{1}{2\sqrt{g}}$ is measured from the Weyl node.

This solution, although formally of zero energy, is not normalizable. On the other hand, it can be expanded in powers of $\sqrt{g}$ to produce the nth-order perturbation theory result for (10), implying that perturbatively $\epsilon_0^{(n)} = 0$. Non-normalizability of this solution implies that there exist nonperturbative contributions to the ground-state energy, since operator $Q^+ Q$ is semipositive.

Let us first discuss the zeroth level. In order to find a nonperturbative correction, we resort to standard Wentzel-Kramers-Brillouin (WKB) technique (see the Supplemental Material [35] for details and a related discussion in Ref. [38]) and obtain for the zeroth level,

$$\epsilon_0 = \sqrt{\frac{\zeta}{\pi}} e^{-1/6g}, \quad (13)$$

to recover the ground-state energy (2). Result (2) is valid up to $g < \frac{1}{4}$ (i.e., for magnetic fields up to B_0) with an error of less than 3%. Higher levels are shifted by the anharmonicity of the potential and splitted according to

$$\epsilon_{2k} - \epsilon_{2k-1} = \sqrt{\frac{\zeta}{\pi}} \left(\frac{2}{g}\right)^k \frac{e^{-1/6g}}{k!}, \quad k \in \mathbb{N}_+. \quad (14)$$

In Eqs. (13) and (14) only the leading term in the semiclassical expansion is retained.

Finally, let us consider intermediate values of angle η. We numerically computed the LL dependence on the longitudinal (along the magnetic field) momentum $\varepsilon(k_\parallel)$ (see Fig. 3). One observes an interesting crossover from a field-independent level at $\eta = 0$ [Eq. (6)] to a level, weakly depending on the magnetic field [Eq. (9)].

For arbitrary η we define the effective gap as an energy of the transversal motion at the Weyl node $\Delta_{\mathrm{eff}} \equiv \varepsilon_0(k_\parallel = k_0 \cos\eta)$. It vanishes at $\eta = 0$ and attains its maximal value at $\eta = \pi/2$. The evolution of Δ_{eff} with η is shown in Fig. 4.

III. MAGNETOCONDUCTANCE

We now evaluate the conductance in the presence of a magnetic field perpendicular to the p-n junction. We will make use of the Landauer formalism and solve the scattering problem for electrons moving from conductance to a valence band through the p-n junction.

For $\eta = 0$ in the transversal motion there exists a field-independent mode [see Eq. (6)]. After substitution $\psi \mapsto \frac{1}{\sqrt{2}}(1 + i\sigma_y)\psi$ and separation of variables $\psi^{1,2}(x,y) = \psi_n^{1,2}(y)\phi^{1,2}(x)$ with functions ψ_n given by (5), the scattering
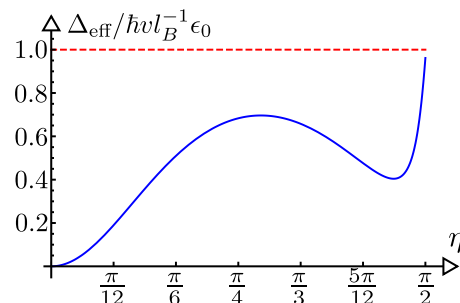
FIG. 4. Effective gap Δ_{eff} as a function of orientation η.

problems reads

$$\left[\frac{\hbar^2 \left(\hat{k}_x^2 - k_0^2 \right)}{2m} \sigma_z + \frac{\hbar v}{l_B} \sqrt{2n} \sigma_x + U(x) \right] \phi = \varepsilon \phi. \quad (15)$$

The potential $U(x)$ is determined by the dopant density deep in the doping region. The relevant screening problem was discussed in Ref. [20]. For numerical estimates, below we will consider the case of moderate doping, $\epsilon_F \gtrsim \Delta$, where ϵ_F is a doping level [for Δ, see Eq. (1)].

The transmission coefficient for the zeroth level is B independent and for a smooth potential is $T_0 \approx 1$ (the slight suppression from unity is due to internode scattering induced by the built-in electric field). After accounting for LL degeneracy this results in a linear contribution to magnetoconductance, $G(B) \propto (e^2/h)(BS/\Phi_0)T_0$, $l_B \ll l_E$, where S stands for the area of the junction. Thus, for $\eta = 0$ the presence of a second nearby Weyl node does not change the magnetoconductance qualitatively, as long as the built-in electric field does not transfer particles between the nodes.

The situation is very different for the junction perpendicular ($\eta = \frac{\pi}{2}$) to $\mathbf{k}_0$. Longitudinal (z) and transverse (x, y) variables can be again separated in the Landau gauge $\mathbf{A} = (-By, 0, 0)$. Substitution $\psi^{1,2} = e^{ik_x x} \chi_n^{1,2}(y l_B^{-1} - \hat{k}_x l_B) \phi^{1,2}(z l_E^{-1})$ leads to transverse equations which are the same as (8), and the following scattering problem,

$$[(-i \partial_z)\sigma_z + (l_E/l_B)\epsilon_n \sigma_x + z]\phi(z) = 0, \quad (16)$$

where we linearized the potential $U(z) = -eEz$ in the vicinity of the crossing points. The problem is equivalent to the Landau-Zener one [39] with the transmission coefficient $T = \exp\left[-\pi(l_E/l_B)^2 \epsilon_n^2\right]$.

Producing a summation over Landau levels,

$$G(B) = \frac{e^2}{h} \frac{S}{2\pi l_B^2} \sum_{\epsilon_n} \exp\left[-\pi \frac{l_E^2}{l_B^2} \epsilon_n^2\right], \quad (17)$$

where we set $\epsilon_n \approx \sqrt{2\zeta n}$ for $n > 0$ and use Eq. (13) for ϵ_0, we obtain the dependence $G(B)$ depicted in Fig. 1,

$$G(B) = 2\pi G_0 b \left[\exp\left(-be^{-\frac{4}{3}\frac{a}{b}}\right) + \frac{\exp(-\pi b)}{2\sinh(\pi b)} \right], \quad (18)$$

where we have introduced

$$G_0 \equiv \frac{2}{\zeta} \frac{e^2}{h} \frac{S}{(2\pi l_E)^2}, \quad a \equiv (\zeta k_0 l_E)^2, \quad b \equiv \zeta \frac{l_E^2}{l_B^2}. \quad (19)$$

In the two-cone model magnetoconductance has a maximum at the magnetic field given by Eq. (3), whose dependence is pictured in Fig. 1.

To test the feasibility of the found results we take numerical values for TaAs [8] and TaP [9,30] and estimate the critical parameters. We suppose doping is weak enough to estimate $E \simeq \Delta^2/(\hbar v)^{3/2}$ according to Ref. [20].

TABLE I. Numerical values, taken from Ref. [8] for TaAs, and Refs. [9,30] for TaP.

	TaAs (W2)	TaP (W1)
$2k_0$ (Å^{-1})	0.0183	0.021
Δ (meV)	2	$\lesssim 2$
$\zeta = v_x/v_y$	1.65	1.6
l_E (Å)	470	720
B_0 (T)	9	11
B_c (T)	3	3.7

The numbers presented in Table I show that the situation we consider is indeed possible in an experimental setup. As $B_c < B_0$, the effective coupling constant g corresponding to the position of the maximum is indeed small and our WKB calculation is valid for such fields.

IV. CONCLUSIONS

To conclude, we have studied the LL structure in WSM analytically ($\eta = 0, \pi/2$) and numerically ($0 < \eta < \pi/2$). Our analytical results are summarized in Eqs. (2) and (3) as well as Fig. 3. We believe that the predicted gap in the LL spectrum has already been observed in the experiment in Ref. [30].

We found that the tunneling between Weyl nodes leads to the appearance of the characteristic field B_c [Eq. (3)] at which the differential magnetoconductance changes its sign. We believe the same feature would exist at intermediate angles, but due to the absence of a separation of longitudinal and transversal motion at $0 < \eta < \pi/2$ in the two-cone approximation, we were not able to study this problem in more detail.

In our treatment, we have completely discarded the influence of disorder and interaction. It means that the characteristic traversal time through a p-n junction should be smaller than the quasiparticle relaxation time. The transport relaxation time in TaAs was estimated in, i.e., Ref. [40], $\tau = 7 \times 10^{-13}$ s and $v_F \approx 0.5 \times 10^6$ m/s. Then the width of the p-n junction should be less than ~ 1 μm. We have also neglected the Zeeman splitting which is negligible as long as the magnetic field is smaller than the spin-orbit interaction scale which produces the spin-orbit splitting of the quasiparticle bands. For TaAs the corresponding magnetic field is estimated [41,42] to be around 50 T. Therefore there exists plenty of space for purely orbital magnetic-induced tunneling in the framework of low-energy Hamiltonian Eq. (1).

Overall, we are positive that the analysis undertaken helps to shed some light on the structure of a realistic WSM in moderate and strong magnetic fields, and hope that the predicted behavior of magnetoconductance of p-n junctions is going to be measured in future experiments.

[1] C. L. Kane and E. J. Mele, Phys. Rev. Lett. **95**, 146802 (2005).

[2] X. Wan, A. M. Turner, A. Vishwanath, and S. Y. Savrasov, Phys. Rev. B **83**, 205101 (2011).

[3] A. A. Burkov and L. Balents, Phys. Rev. Lett. **107**, 127205 (2011).

[4] A. A. Burkov, M. D. Hook, and L. Balents, Phys. Rev. B **84**, 235126 (2011).

[5] G. B. Halász and L. Balents, Phys. Rev. B **85**, 035103 (2012).

[6] O. Vafek and A. Vishwanath, Annu. Rev. Condens. Matter Phys. **5**, 83 (2014).

[7] B. Q. Lv, H. M. Weng, B. B. Fu, X. P. Wang, H. Miao, J. Ma, P. Richard, X. C. Huang, L. X. Zhao, G. F. Chen, Z. Fang, X. Dai, T. Qian, and H. Ding, Phys. Rev. X **5**, 031013 (2015).

[8] B. Q. Lv, N. Xu, H. M. Weng, J. Z. Ma, P. Richard, X. C. Huang, L. X. Zhao, G. F. Chen, C. E. Matt, F. Bisti, V. N. Strocov, J. Mesot, Z. Fang, X. Dai, T. Qian, M. Shi, and H. Ding, Nat. Phys. **11**, 724 (2015).

[9] N. Xu, H. M. Weng, B. Q. Lv, C. E. Matt, J. Park, F. Bisti, V. N. Strocov, D. Gawryluk, E. Pomjakushina, K. Conder, N. C. Plumb, M. Radovic, G. Autès, O. V. Yazyev, Z. Fang, X. Dai, T. Qian, J. Mesot, H. Ding, and M. Shi, Nat. Commun. **7**, 11006 (2016).

[10] H. Weng, C. Fang, Z. Fang, B. A. Bernevig, and X. Dai, Phys. Rev. X **5**, 011029 (2015).

[11] S.-M. Huang, S.-Y. Xu, I. Belopolski, C.-C. Lee, G. Chang, B. Wang, N. Alidoust, G. Bian, M. Neupane, C. Zhang, S. Jia, A. Bansil, H. Lin, and M. Z. Hasan, Nat. Commun. **6**, 7373 (2015).

[12] S. Jeon, B. B. Zhou, A. Gyenis, B. E. Feldman, I. Kimchi, A. C. Potter, Q. D. Gibson, R. J. Cava, A. Vishwanath, and A. Yazdani, Nat. Mater. **13**, 851 (2014).

[13] J. Xiong, S. K. Kushwaha, T. Liang, J. W. Krizan, M. Hirschberger, W. Wang, R. J. Cava, and N. P. Ong, Science **350**, 413 (2015).

[14] Q. Li, D. E. Kharzeev, C. Zhang, Y. Huang, I. Pletikosić, A. Fedorov, R. Zhong, J. Schneeloch, G. Gu, and T. Valla, Nat. Phys. **12**, 550 (2016).

[15] J. Xiong, S. K. Kushwaha, T. Liang, J. W. Krizan, W. Wang, R. J. Cava, and N. P. Ong, arXiv:1503.08179.

[16] F. Arnold, C. Shekhar, S.-C. Wu, Y. Sun, R. D. Dos Reis, N. Kumar, M. Naumann, M. O. Ajeesh, M. Schmidt, A. G. Grushin, J. H. Bardarson, M. Baenitz, D. Sokolov, H. Borrmann, M. Nicklas, C. Felser, E. Hassinger, and B. Yan, Nat. Commun. **7**, 11615 (2016).

[17] C. M. Wang, H.-Z. Lu, and S.-Q. Shen, Phys. Rev. Lett. **117**, 077201 (2016).

[18] D. T. Son and B. Z. Spivak, Phys. Rev. B **88**, 104412 (2013).

[19] J. Klier, I. V. Gornyi, and A. D. Mirlin, Phys. Rev. B **92**, 205113 (2015).

[20] S. Li, A. V. Andreev, and B. Z. Spivak, Phys. Rev. B **94**, 081408 (2016).

[21] B. Z. Spivak and A. V. Andreev, Phys. Rev. B **93**, 085107 (2016).

[22] L. P. He, X. C. Hong, J. K. Dong, J. Pan, Z. Zhang, J. Zhang, and S. Y. Li, Phys. Rev. Lett. **113**, 246402 (2014).

[23] Y. Zhao, H. Liu, C. Zhang, H. Wang, J. Wang, Z. Lin, Y. Xing, H. Lu, J. Liu, Y. Wang, S. M. Brombosz, Z. Xiao, S. Jia, X. C. Xie, and J. Wang, Phys. Rev. X **5**, 031037 (2015).

[24] M. Novak, S. Sasaki, K. Segawa, and Y. Ando, Phys. Rev. B **91**, 041203 (2015).

[25] J. H. Du, H. D. Wang, Q. Chen, Q. H. Mao, R. Khan, B. J. Xu, Y. X. Zhou, Y. N. Zhang, J. H. Yang, B. Chen, C. M. Feng, and M. H. Fang, Sci. China: Phys. Mech. Astron. **59**, 657406 (2016).

[26] L. V. Keldysh, Zh. Eksp. Teor. Fiz. **33**, 994 (1958).

[27] A. G. Aronov and G. E. Pikus, Zh. Eksp. Teor. Fiz. **51**, 281 (1967).

[28] L. Esaki and R. R. Haering, J. Appl. Phys. **33**, 2106 (1962).

[29] H. Nielsen and M. Ninomiya, Phys. Lett. B **130**, 389 (1983).

[30] C.-L. Zhang, S.-Y. Xu, C. M. Wang, Z. Lin, Z. Z. Du, C. Guo, C.-C. Lee, H. Lu, Y. Feng, S.-M. Huang, G. Chang, C.-H. Hsu, H. Liu, H. Lin, L. Li, C. Zhang, J. Zhang, X.-C. Xie, T. Neupert, M. Z. Hasan, H.-Z. Lu, J. Wang, and S. Jia, Nat. Phys. **13**, 979 (2017).

[31] R. Okugawa and S. Murakami, Phys. Rev. B **89**, 235315 (2014).

[32] T. E. O'Brien, M. Diez, and C. W. J. Beenakker, Phys. Rev. Lett. **116**, 236401 (2016).

[33] C.-K. Chan and P. A. Lee, Phys. Rev. B **96**, 195143 (2017).

[34] P. Kim, J. H. Ryoo, and C.-H. Park, Phys. Rev. Lett. **119**, 266401 (2017).

[35] See Supplemental Material at http://link.aps.org/supplemental/10.1103/PhysRevB.97.041202. for derivation of the expression for zeroth LL using the WKB technique and an illustration of the magnetic field orientation.

[36] H.-Z. Lu, S.-B. Zhang, and S.-Q. Shen, Phys. Rev. B **92**, 045203 (2015).

[37] L. E. Gendenshtein and I. V. Krive, Usp. Fiz. Nauk **146**, 553 (1985).

[38] Y. V. Fyodorov, P. L. Doussal, A. Rosso, and C. Texier, arXiv:1703.10066.

[39] A. V. Shytov, N. Gu, and L. S. Levitov, arXiv:0708.3081.

[40] C.-L. Zhang, S.-Y. Xu, I. Belopolski, Z. Yuan, Z. Lin, B. Tong, N. Alidoust, C.-C. Lee, S.-M. Huang, T.-R. Chang et al., Nat. Commun. **7**, 10735 (2016).

[41] F. Arnold, M. Naumann, S.-C. Wu, Y. Sun, M. Schmidt, H. Borrmann, C. Felser, B. Yan, and E. Hassinger, Phys. Rev. Lett. **117**, 146401 (2016).

[42] B. J. Ramshaw, K. A. Modic, A. Shekhter, Y. Zhang, E.-A. Kim, P. J. W. Moll, M. Bachmann, M. K. Chan, J. B. Betts, F. Balakirev et al., arXiv:1704.06944.